Mon. Not. R. Astron. Soc. **341,** 760–770 (2003)

Modelling the high-eccentricity planetary three-body problem. Application to the GJ876 planetary system

C. Beaugé[1]★† and T. A. Michtchenko[2]

[1]*Observatorio Astronómico, Universidad Nacional de Córdoba, Laprida 854, (X5000BGR) Córdoba, Argentina*
[2]*Instituto de Astronomia, Geofísica e Ciências Atmosféricas, USP, Rua do Matão 1226, 05508-900 São Paulo, Brazil*

Accepted 2002 December 10. Received 2002 December 3; in original form 2002 July 26

ABSTRACT

The discovery of extrasolar planets located in the vicinity of mean-motion commensurabilities has opened a new arena for the study of resonance capture and its possible role in the dynamical evolution and long-term stability of planetary systems. Contrary to our own Solar System, many of these planets have highly eccentric orbits (∼0.1–0.6), making the use of usual analytical perturbative models very limited. Even so, several attempts have been made to apply classical expansions of the resonant Hamiltonian to these cases, leading to results which are, at best, extrapolations of the low-eccentricity resonant structure, and not necessarily precise.

In this paper we present a new analytical expansion for the Hamiltonian of the planetary three-body problem which does not suffer these restrictions, and is even valid for crossing orbits. The only limitation is its applicability to planar motions. The resulting model can be applied to resonant and non-resonant configurations alike. We show examples of this expansion in different resonances and we compare the results with numerical determinations of the exact Hamiltonian.

Finally, we apply the developed model to the case of two planets in the 2/1 mean-motion commensurability (such as the Gliese 876 system), and we analyse its periodic orbits and general structure of the resonant phase space at low and high eccentricities.

Key words: methods: analytical – celestial mechanics – planets and satellites: general – planetary systems.

1 INTRODUCTION

The discovery of extrasolar planets in mean-motion commensurabilities has opened a whole new arena for the study of the planetary three-body problem. Among others, we can mention the search for equilibrium solutions, the study of mechanisms of resonance trapping, as well as the existence of stable and chaotic regions of the phase space for different values of the planetary masses and initial conditions. Thus, many of the techniques and models derived for the study of our own Solar System are now being modified and applied to new scenarios and new objects. The aim, however, remains the same: to analyse what role (if any) resonances could play in the origin and stability of the observed configuration of the planetary systems.

Marcy et al. (2001) discovered that the two planets orbiting Gliese 876 are locked in a 2/1 mean-motion resonance, and they suggested that this commensurability may in fact be responsible for the orbital stability of the system. Numerical simulations seem to indicate that these bodies are actually trapped in what celestial mechanicians call a 'corotation point'. Unlike the term 'corotation resonance' widely used in the context of planet–disc interactions, a corotation point is a stationary solution of the averaged resonant system. In other words, the bodies exhibit a simultaneous libration of the resonant angle and an alignment of their major axes (Laughlin & Chambers 2001; Lee & Peale 2002). Another extrasolar planetary system, HD 82943, also seems to have two planets in a 2/1 commensurability relation (Butler et al. 2002), although in this case it is unclear whether the observed motion is also a corotation or a simple libration of the resonant angle. Finally, there is evidence that the second body recently discovered in 47 Uma (Fischer et al. 2002) may be close to the 5/2 resonance with 47 Uma-b.

Several studies have been performed in the past couple of years on the origin and stability of these resonant systems. Among these, we can mention Ford, Havlikova & Rasio (2001), Murray, Paskowitz & Holman (2002), Hadjidemetriou (2002), Lee & Peale (2002), and others. Several of these have the aim of finding initial conditions and masses that yield stable solutions. Because the observational data usually do not yield explicit values for the masses, these tests are very important in determining upper bounds for these parameters, as well as indications for the inclination of the orbital plane of the planetary system.

★E-mail: beauge@oac.uncor.edu
†Present address: Instituto Nacional de Pesquisas Espaciais, Av. dos Astronautas 1758, (12227-010) São José dos Campos, SP, Brazil.

Hadjidemetriou (2002) studied the stability of numerically generated families of periodic orbits in the planar-elliptic 2/1 resonance, and applied the results to both the Gliese 876 and the HD 82943 systems. He found that, in such a commensurability, all solutions are unstable if: (i) the mass of the outer planet is smaller than the mass of the inner body, or (ii) the eccentricity of the outer body is larger than that of the inner planet. In particular, his results indicate that both observed planetary systems are close to stable periodic solutions and thus seem to be dynamically stable.

Although most of the works have been numerical in nature, there has also been a recent attempt to develop analytical models for these systems. Among the first, Murray et al. (2002) analysed the process of resonance capture in a scenario where both planets lose energy and angular momentum due to unspecified external dissipative forces. They have shown that in certain cases the inward migration of the bodies can lead to a substantial increase in their eccentricities, yielding values of the same order as those observed in the real systems. The analytical model used was based on a Laplacian type expansion of the resonant Hamiltonian (see Holman & Murray 1996), although many of their results should be independent of the particular expression adopted for this function.

A more detailed model was recently developed by Lee & Peale (2002), who presented a very complete study on the capture of these planets into the resonance by the inward migration due to interaction with a gaseous or planetesimal disc. This capture may not only explain the present corotation configuration, but also the large eccentricity shown by both planets. Once again, the model was based on a Laplacian expansion of the disturbing function, truncated at third order in the eccentricities. The resulting equations were then used to discuss the existence and locations of equilibrium solutions in the averaged (resonant) phase space of the system.

In both these works, the analytical model was not fundamental to their results and was used only to obtain qualitative information. However, it is important to keep in mind that, for the 2/1 resonance, the Laplace expansion is not convergent for eccentricities above $\sim$0.17 (see Ferraz-Mello 1994), and low-order truncated expressions yield quantitatively imprecise results much sooner. This limit may not be significant in the case of our own Solar System where the planets move in quasi-circular orbits, but the same does not hold for extrasolar systems. In the case of Gliese 876, the eccentricities of the planets are approximately 0.12 and 0.27. For HD 82943 it is even worse, as these values are of the order of 0.41 and 0.54. So, for both these resonant pairs, the adopted analytical model is not recommended and a new expansion must be used. In fact, in many cases even truncated classical models may lead to incorrect qualitative results. It is well known (see Beaugé 1994) that low-order expansions may predict a structure for the phase space (such as equilibrium solutions or stability index) which do not correspond to the real system.

The aim of the present work is precisely to develop an expansion of the Hamiltonian of the planetary three-body problem which does not have these limitations and can be applied to the case of high-eccentricity orbits. It is based on the so-called global expansion of the disturbing function (Beaugé 1996), originally developed for the restricted three-body problem with quasi-circular perturbers. Here we present a variation of this function which contains several improvements, including a much more simplified method for the calculation of the coefficients. The resulting expansion can be applied to any generic mean-motion commensurability or even to the case of non-resonant orbits. In this paper, the expansion will be restricted to planar motions, although an extension to the spatial case will be presented in the near future.

This paper is divided as follows. In Section 2 we introduce the dynamical variables of the system and sketch the generic form of the Hamiltonian function. In Section 3 we present the expansion of the disturbing function for the general three-body problem. The case of a generic mean-motion resonance for both planets is discussed in Section 4, together with some comparisons with numerical calculations. In Section 5 we apply the resulting model to the case of the 2/1 resonance, and we analyse the results. Finally, discussions and future applications of the model are approached in Section 6.

2 THE HAMILTONIAN IN POINCARÉ VARIABLES

Suppose three bodies of finite mass M_0, m_1 and m_2 orbiting their common centre of mass, with $M_0 \gg m_1, m_2$ and $m_1, m_2 > 0$. M_0 is to be the star of our system, and m_i the planets. Of course this is just an example, and the same dynamical system could be said to represent the problem of two massive satellites orbiting a planet. However, as we primarily apply the model to extrasolar planetary systems, we use the first physical scenario throughout this work.

We define the following set of canonical variables:

$$\begin{aligned} &\lambda_i; \quad L_i &&= m'_i\sqrt{\mu_i a_i} \\ &\varpi_i; \quad G_i - L_i &&= -L_i\left(1-\sqrt{1-e_i^2}\right) \\ &\Omega_i; \quad H_i - G_i &&= -L_i\sqrt{1-e_i^2}\,(1-\cos I_i) \end{aligned} \tag{1}$$

where a_i, e_i, I_i, λ_i, ϖ_i and Ω_i are the orbital elements of the ith planet ($i = 1, 2$), $\mu_i = \kappa^2 (M_0 + m_i)$, κ is the Gaussian gravitational constant, and m'_i is a reduced mass given by

$$m'_i = \frac{m_i M_0}{m_i + M_0}. \tag{2}$$

These are the so-called Poincaré variables, and correspond to a variant of the modified Delaunay canonical set (see Laskar 1991). The Hamiltonian F of the system can be expressed as a sum of two terms

$$F = F_0 + F_1 \tag{3}$$

where the first corresponds to the two-body contribution, and is given by

$$F_0 = -\sum_{i=1}^{2} \frac{\mu_i^2 m'^3_i}{2L_i^2}. \tag{4}$$

The second term, F_1, is the disturbing function of the problem. According to Laskar (1991), it can be expressed as

$$F_1 = -\kappa^2 m_1 m_2 \frac{1}{\Delta} + T_1, \tag{5}$$

where Δ is the instantaneous distance between both planets and T_1 is the indirect part of the potential function. In terms of the heliocentric Cartesian coordinates (x_i, y_i, z_i) of each mass, up to the first order in the masses this latter function has the form:

$$T_1 = \frac{m_1 m_2}{M_0}(\dot{x}_1\dot{x}_2 + \dot{y}_1\dot{y}_2 + \dot{z}_1\dot{z}_2). \tag{6}$$

Here $\dot{x}_i$ denotes the temporal derivative of x_i and, obviously, the same notation holds for the remaining coordinates. The reader is referred to Laskar (1991) and Laskar & Robutel (1995) for further details.

The Hamiltonian of the planetary version of the three-body problem has two main differences with respect to the restricted case: (i) a factor proportional to the mass in the unperturbed contribution, and

(ii) a different aspect for the indirect part of the disturbing function, which now depends on the velocity components and not on the coordinates. This second modification is very significant and implies that the expansions of both the direct and indirect terms cannot be unified in a single expression.

3 EXPANSION OF THE DISTURBING FUNCTION

As mentioned in the introduction, we wish to develop an expression for the Hamiltonian F which is valid in the case where one or both of the planets may exhibit high eccentricities, and possibly even have overlapping orbits. In such configurations, classical expansions such as Laplace (1799) or Kaula (1962) are not adequate; see also Duriez (1988) and Ellis & Murray (2001) for more recent variations. For eccentricities below the apocentric collision point, these series are either divergent, as in the case of Laplace expansion above the Sudmann curve (see Ferraz-Mello 1994) or they converge very slowly to the point of needing literally millions of terms to reproduce the exact function with even moderate precision. For eccentricities above the collision point, all these classical expansions are useless.

A few years ago, Beaugé (1996) presented a new 'global' expansion of the disturbing function which did not have these limitations. In principle, it converges (although conditionally) in all points of the phase space not including the singularities associated with collisions between both bodies. The rate of convergence, and thus the number of terms necessary for a given precision of the model, does not depend explicitly on the eccentricities of the bodies or the angular variables chosen as initial conditions. In fact, it is mainly a function of the value of the disturbing function itself. Thus, initial conditions for which the value of F_1 is relatively small (such as in the vicinity of a corotation point, or very far from the perturber) need only a few terms in order to reproduce it adequately. On the other hand, initial conditions close to the collision point (thus yielding very high values of F_1) need a large number of terms.

Although this expansion proved to be formally very simple, it had very limited applicability to concrete problems, and was in fact more interesting in an academic sense than from the practitioner's point of view. This was due to two reasons. (i) Because the objective was to obtain a series expansion valid for any eccentricity, many of the intermediate expansions were undertaken via complex functions with little or no recurrence relations, and which implied a very costly determination in terms of CPU time. (ii) The expansion was constructed around the restricted three-body problem and, moreover, the perturber was supposed to move in a quasi-circular orbit.

If we hope to adapt this expansion to the problem at hand, we must solve these limitations. This will be the aim of this section. On one hand, we present simpler intermediate expansions in terms of Newcomb operators, and the expansion is re-constructed for the case of a high-eccentricity perturber. Finally, it is also important to mention that the original expansion was limited to two dimensions. In other words, the motion of all bodies was supposed to occur in a plane. Although this limitation is important for studies in asteroidal dynamics, it is not very restrictive in the case of extrasolar planets. In most cases, the mutual inclination of these bodies is completely unknown and therefore usually assumed to be zero.

3.1 The direct part of F_1 and the parameter δ

As usual, we begin discussing the direct part of the disturbing function, which contains the main problems in convergence. In terms of the heliocentric radial distances r_i of both planets, we can write it as

$$\frac{1}{\Delta} = \left(r_1^2 + r_2^2 - 2r_1 r_2 \cos S\right)^{-1/2} \tag{7}$$

where $S = f_1 - f_2 + \Delta\varpi$ is the angle between both bodies as seen from the central mass, f_i are the true anomalies, and $\Delta\varpi = \varpi_1 - \varpi_2$ is the difference in longitudes of perihelia. Introducing the ratio $\rho = r_1/r_2$, we can rewrite equation (7) in a more treatable form as

$$\frac{r_2}{\Delta} = (1 + \rho^2 - 2\rho \cos S)^{-1/2}. \tag{8}$$

Instead of expanding this function in Fourier series of S or power series of ρ (as commonly used in classical approaches), here we choose a different route. Defining $x = \rho^2 - 2\rho \cos S$, we can write

$$\frac{r_2}{\Delta} = (1 + x)^{-1/2}. \tag{9}$$

This is the key of our method. The expression of the direct part of the disturbing function has gained in simplicity, as the number of pertinent variables has been reduced to one. The variable x is a measure of the proximity of the initial condition to the singularity in $1/\Delta$. It is equal to -1 at the pole, and takes values larger than this for every point $(\rho, \cos S)$ outside the collision point. Notice that the magnitude of ρ or the value of S are not intrinsically significant to the disturbing function, only the distance from the singularity is actually important.

In this manner, the problem of the expansion of $1/\Delta$ has been reduced to that of the function $(1 + x)^{-1/2}$, and the convergence is thus independent of ρ. In Beaugé (1996) this function was expanded via a Taylor series in x around the point $x = 0$. This is a good solution for initial conditions close to the origin, but implies a huge number of terms if we wish to analyse values of x far from zero. Because in this work we are interested in practical applications, it is important to reduce the number of terms to a minimum. We must then search for a different approach. A solution is to approximate $(1 + x)^{-1/2}$ by a linear fit in powers of x. In other words, we express

$$(1 + x)^{-1/2} \simeq \sum_{n=0}^{N} b_n x^n \tag{10}$$

by a polynomial of order N, where the coefficients b_n are determined numerically via a linear regression. As the original function has a singularity at $x = -1$, this point must be excluded from our data. Thus, the numerical fit is performed using values of $x > -1 + \delta$, where δ is a positive parameter close to zero. The smaller its value, the better the approximation to the real function near the singularity. However, the smaller the value of δ, the larger the value of N will have to be in order to guarantee an adequate precision for all values of the independent variable.

In practice, a compromise must be reached. The adopted value of δ will depend on two factors: first, the mean-motion resonance and/or the region of the phase space of interest; secondly, the degree of precision desired of the expansion. Fig. 1 shows the relative error of equation (10) for $N = 30$ and two values of δ. The solid line represents the case of $\delta = 0.1$ while the dashed line represents the case $\delta = 0.01$. We can see that for most of the interval of x, this larger value of δ yields a much higher precision, and the error lies in the order of 10^{-6}. This is about three orders of magnitude lower than in the other case. Conversely, as $x \to -1$, the fit with $\delta = 0.01$ is much more precise. Of course, larger values of N will diminish the error in both cases, but at the cost of increasing the number of terms enormously.

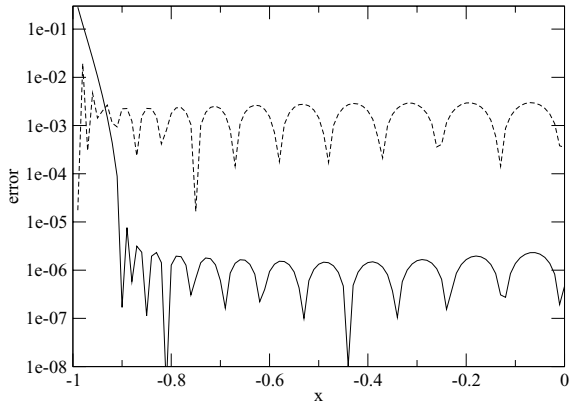

Figure 1. Relative error of the approximation given by equation (10) and the original function $1/\sqrt{1+x}$, as a function of x, for two values of δ. The continuous line shows the case $\delta = 0.1$ and the dashed line shows $\delta = 0.01$. In both examples, we chose $N = 30$.

The question is now how to relate a given interval in x with concrete initial conditions for the three-body problem. In other words, given a certain configuration for both planets, what interval of values of x can we expect?

Imagine that both planets m_i lie in the vicinity of a generic mean-motion commensurability $(p + q)/p$. Then, we can define $q\sigma_i = (p + q)\lambda_2 - p\lambda_1 - q\varpi_i$, with $i = 1, 2$, as the two resonant angles of the system. Let us consider the simplest case and suppose that the eccentricity of the exterior body is set to zero (i.e. $e_2 = 0$), and set the semimajor axes such that their ratio is equal to exact resonance. In this scenario, let us consider all the possible initial angular variables of the problem that yield a certain value of $(k, h) = e_1(\cos q\sigma_1, \sin q\sigma_1)$. For each of these initial conditions, we calculate x and determine its minimum value $x_{\min}$. This gives us as a final product a set $(k, h, x_{\min})$ for each resonance. The result can now be plotted in the form of a grey-scale graph of equal value of $x_{\min}$. This is shown in Fig. 2 for four different commensurabilities. The broad white lines, observed in all but the 3/1 resonance, mark the location of the collision curve, which is identified as those points where $x_{\min} = -1$.

It can be easily shown that the geometry of the level curves follows very closely the topology of the resonant phase plane, averaged over short-period terms. In other words, there seems to be a direct link between the value of $x_{\min}$ and the averaged resonant disturbing function $\langle R \rangle$. The maximum value of $x_{\min}$ lies in the apsidal axis (i.e. $h = 0$) and corresponds to the minimum of $\langle F_1 \rangle$. This value is related to the corotation point of the resonance and, thus, to the equilibrium solution of the commensurability. Notice that this corotation may occur for eccentricities higher than that for which orbital overlap is possible. The minimum value of $x_{\min}$ (equal to -1) corresponds to the singularities of $\langle F_1 \rangle$.

We can also note that there is no direct relationship between the eccentricity and $x_{\min}$. A small amplitude librating orbit with a large eccentricity may have a large value of $x_{\min}$, while a quasi-circular orbit may have a value very close to -1. In principle this is not a good thing, as it means that an expansion of the disturbing function may yield a better precision for high eccentricities than for circular orbits. However, it does have the advantage that it guarantees that the same expansion will have a minimum error in precisely the region of the phase space where most of the resonant orbits are located. More importantly, as we are approximating the function $1/\Delta$ by a truncated polynomial in x, this expansion will have no singularities.

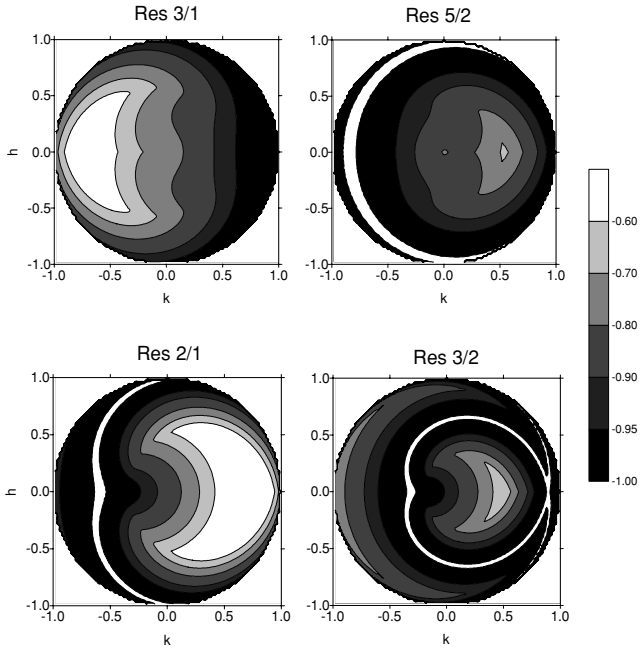

Figure 2. Level curves of $x_{\min}$ in the plane $(k, h) = e_1(\cos q\sigma_1, \sin q\sigma_1)$ for four different mean-motion resonances.

This means that our expansion will be valid for all values of the eccentricities or semimajor axes, although it may underestimate the true function close to the collision curve.

Possibly the greatest advantage of using x as a parameter of the expansion lies in the fact that it is a variable of the three-body problem, and not of the two-body problem. Depending on the angles, a given e_i or $\alpha = a_1/a_2$ may yield any value of F_1, from a local minimum of the function to a singularity. This problem does not occur in our case, making x much more adequate.

Summarizing then, if we are interested in studying systems located at low eccentricities, the expansion developed in this paper is possibly not the best option, and usual methods are recommended. However, if the problem may present high eccentricities with a predominance of motions in libration in mean-motion resonances, then this method may be a good choice. It is important to recall that many of the extrasolar planet pairs observed in resonant configuration lie precisely in the region of the corotation point, where $x_{\min}$ is maximum and the error of the present expansion is minimum.

In view of these discussions, and as we are not interested in solutions very close to the collision curve, we need not consider a very small value of δ for our expansion. In all the following calculations, we choose $\delta = 0.1$ and $N = 30$. This guarantees a precision of about 10^{-6} in the polynomial expansion of equation (2), although it does mean that the expansion underestimates the value of the perturbation near the collision curve.

Having finally opted for values of these parameters, we can return to our expansion. Introducing the explicit expression for x into equation (10), we can write the truncated series as

$$\frac{r_2}{\Delta} \simeq \sum_{k=0}^{N} \sum_{j=0}^{n} c_k (-2)^j \binom{k}{j} \rho^{2k-j} \cos^j S \qquad (11)$$

where c_k are constant coefficients, easily obtainable in terms of the original b_k. Changing from powers of the cosines to multiples of the argument, we can rewrite this as

$$\frac{a_2}{\Delta} \simeq \sum_{k=0}^{N} \sum_{i=0}^{N-k} 2A_{k,i}\alpha^m \left(\frac{r_1}{a_1}\right)^m \left(\frac{r_2}{a_2}\right)^{-m-1} \cos kS \tag{12}$$

where $m = 2i + k$. Expanding S and passing from trigonometric functions to their exponential counterparts, we obtain

$$\begin{aligned}\frac{a_2}{\Delta} \simeq & \sum_{k=0}^{N} \sum_{i=0}^{N-k} A_{k,i}\alpha^m \\ & \times \left[\left(\frac{r_1}{a_1}\right)^m \mathrm{E}^{\sqrt{-1}kf_1} \left(\frac{r_2}{a_2}\right)^{-m-1} \mathrm{E}^{-\sqrt{-1}kf_2} \mathrm{e}^{\sqrt{-1}k\Delta\varpi} \right. \\ & \left. + \left(\frac{r_1}{a_1}\right)^m \mathrm{E}^{-\sqrt{-1}kf_1} \left(\frac{r_2}{a_2}\right)^{-m-1} \mathrm{E}^{\sqrt{-1}kf_2} \mathrm{e}^{-\sqrt{-1}k\Delta\varpi} \right]. \end{aligned} \tag{13}$$

This constitutes the final expression of the direct part of the disturbing function, as yet in terms of the true angular variables.

3.2 From true to mean angular variables

In the present work, we limit the applicability of the resulting expansion of F_1 in two ways: (i) we disregard the behaviour of the system beyond the collision curve of a given resonance, and (ii) we restrict the eccentricities e_i of the planets to $\sim$0.5. Both these conditions, together with the adoption of the reasonably moderate value for N, allow us to avoid all the complicated transformations introduced in Beaugé (1996) for the passage from f_i to M_i. We can then simplify greatly our work and make use of the well-known Newcomb operators and Hansen coefficients.

Momentarily dropping the subindex in the orbital elements of the body, we can write

$$\begin{aligned}\left(\frac{r}{a}\right)^n \cos(kf) &= \sum_{j=0}^{\infty} \left(X_j^{n,k} + X_{-j}^{n,k}\right) \cos(jM) \\ \left(\frac{r}{a}\right)^n \sin(kf) &= \sum_{j=0}^{\infty} \left(X_j^{n,k} - X_{-j}^{n,k}\right) \sin(jM) \end{aligned} \tag{14}$$

where the n index may be either positive or negative. $X_j^{n,k}$ are called Hansen coefficients and are a function of the eccentricity (e.g. Brouwer & Clemence 1961; Kaula 1962). The coefficients have the following explicit expressions

$$X_j^{n,k} = \mathrm{e}^{|k-j|} \sum_{s=0}^{\infty} Y_{s+u_1,s+u_2}^{n,k} e^{2s} \tag{15}$$

where $u_1 = \max(0,\, j-k)$ and $u_2 = \max(0,\, k-j)$. $Y_{s+u_1,s+u_2}^{n,k}$ are referred to as Newcomb operators. They have the great advantage of having simple recurrence relations (see Kaula 1962) and are thus very easy (and fast) to calculate for any value of the index. Introducing equation (14) into equation (13) and after some simple algebra, we finally obtain

$$\begin{aligned}\left(\frac{r}{a}\right)^n \cos(kf) &= \sum_{i=0}^{\infty} \sum_{m=-\infty}^{\infty} B_{n,k,i,m} e^i \cos(mM) \\ \left(\frac{r}{a}\right)^n \sin(kf) &= \sum_{i=0}^{\infty} \sum_{m=-\infty}^{\infty} C_{n,k,i,m} e^i \sin(mM) \end{aligned} \tag{16}$$

where $B_{n,k,i,m}$ and $C_{n,k,i,m}$ are constant coefficients obtained as function of Newcomb operators. Their advantage with regards to the Hansen coefficients lies in the fact that they are independent of the eccentricity, and thus invariant for all initial conditions. Thus, they only need to be determined once.

As a final step, introducing the transformation (16) into the expansion of the direct part of the disturbing function, and after a cumbersome reordering of the terms, we obtain

$$\begin{aligned}\frac{a_2}{\Delta} \simeq & \sum_{j,k=0}^{\infty} \sum_{m,n=-\infty}^{\infty} \sum_{l=0}^{N} \sum_{i=0}^{N-l} A_{l,i} D_{2i+l,j,k,m,n} \\ & \times \alpha^{2i+l} e_1^i e_2^j \cos(mM_1 - nM_2 + l\Delta\varpi) \end{aligned} \tag{17}$$

where the $D_{2i+l,j,k,m,n}$ coefficients are given by

$$\begin{aligned} D_{2i+l,j,k,m,n} = & \frac{1}{2\gamma_m\gamma_n} (B_{2i+l,l,j,|m|} + \mathrm{sign}(m) C_{2i+l,l,j,|m|}) \\ & \times (B_{-2i-l-1,l,k,|n|} + \mathrm{sign}(n) C_{-2i-l-1,l,k,|n|}) \end{aligned} \tag{18}$$

and where γ_m is a simple bi-valuate function defined as

$$\gamma_m = \begin{cases} 1/2 & \text{if} \quad m = 0 \\ 1 & \text{if} \quad m > 0. \end{cases} \tag{19}$$

In the cases where we are studying the vicinity of mean-motion resonances, it is not worthwhile to maintain the sum in α. It is much better to expand this contribution in a Taylor series around the exact resonances, keeping only two or three orders of the expansion. This, however, will be detailed in the next section.

3.3 The indirect part of the disturbing function

Recall from equation (6) that the indirect part of F_1 is given by a function T_1 which depends on the time derivatives of the Cartesian coordinates. As

$$\dot{x}_i \equiv \frac{\mathrm{d}x_i}{\mathrm{d}t} = \frac{\partial x_i}{\partial M_i} \frac{\mathrm{d}M_i}{\mathrm{d}t} = \frac{\partial x_i}{\partial M_i} n_i, \tag{20}$$

where M_i is the mean anomaly and n_i is the mean motion, the indirect part can be approximately rewritten as

$$\begin{aligned} T_1 = & \kappa^2 m_1 m_2 \alpha^{-1/2} \\ & \times \left[\frac{\partial}{\partial M_1}\left(\frac{x_1}{a_1}\right) \frac{\partial}{\partial M_2}\left(\frac{x_2}{a_2}\right) + \frac{\partial}{\partial M_1}\left(\frac{y_1}{a_1}\right) \frac{\partial}{\partial M_2}\left(\frac{y_2}{a_2}\right) \right]. \end{aligned} \tag{21}$$

We show explicitly the calculations for (x_1/a_1). Those for the other coordinates are analogous. We begin by recalling

$$\begin{aligned} \frac{x_1}{a_1} &= \left(\frac{r_1}{a_1}\right) \cos(f_1 + \varpi_1) \\ &= \frac{1}{2}\left(\frac{r_1}{a_1}\right) \mathrm{E}^{\sqrt{-1}f_1} \mathrm{E}^{\sqrt{-1}\varpi_1} + \frac{1}{2}\left(\frac{r_1}{a_1}\right) \mathrm{E}^{-\sqrt{-1}f_1} \mathrm{E}^{-\sqrt{-1}\varpi_1}. \end{aligned} \tag{22}$$

Introducing the transformation (16), we can write

$$\begin{aligned} \frac{x_1}{a_1} &= \sum_{i=0}^{\infty} \sum_{j=-\infty}^{\infty} I_{i,j} e^i \cos(jM_1 + \varpi_1) \\ \frac{y_1}{a_1} &= \sum_{i=0}^{\infty} \sum_{j=-\infty}^{\infty} I_{i,j} e^i \sin(jM_1 + \varpi_1) \end{aligned} \tag{23}$$

where

$$I_{i,j} = \frac{1}{2\gamma_j} (B_{1,1,i,|j|} + \mathrm{sign}(j) C_{1,1,i,|j|}). \tag{24}$$

Differentiating these equations with respect to the mean anomalies, and introducing the result into T_1, we obtain the following expression:

$$T_1 = \frac{\kappa^2 m_1 m_2}{a_2 \alpha^{1/2}} \sum_{j,k=0}^{\infty} \sum_{m,n=-\infty}^{\infty} mn I_{j,m} I_{k,n} \times e_1^j e_2^k \cos(mM_1 - nM_2 + \Delta\varpi). \quad (25)$$

Notice that, except for the dependence on α, this series has the same aspect as the direct part of F_1. To complete the similarity, we can substitute the factor $\alpha^{-1/2}$ by a power series expansion

$$\alpha^{-1/2} = \sum_{i=0}^{2N} \overline{A}_i \alpha^i \quad (26)$$

where $\overline{A}_i$ are constant coefficients. With this change, T_1 now reads

$$T_1 = \frac{\kappa^2 m_1 m_2}{a_2} \sum_{i=0}^{2N} \sum_{j,k=0}^{\infty} \sum_{m,n=-\infty}^{\infty} \overline{A}_i mn I_{j,m} I_{k,n} \times \alpha^i e_1^j e_2^k \cos(mM_1 - nM_2 + \Delta\varpi) \quad (27)$$

which is the final expression for the indirect potential. As it now has the same functional form as the expansion of $1/\Delta$, we can unify both expressions and obtain a single series for the complete disturbing function of the planetary three-body problem as

$$F_1 = \kappa^2 m_1 m_2 \sum_{j,k=0}^{\infty} \sum_{m,n=-\infty}^{\infty} \sum_{l=0}^{N} \sum_{i=0}^{2N} R_{i,j,k,m,n,l} \times \frac{a_1^i}{a_2^{i+1}} e_1^j e_2^k \cos(mM_1 - nM_2 + l\Delta\varpi) \quad (28)$$

where the final coefficients are given by

$$R_{i,j,k,m,n,l} = A_{l,(i-l)/2} D_{i,j,k,m,n} - \delta_{l,0} \overline{A}_i mn I_{j,m} I_{k,n} \quad (29)$$

where $\delta_{l,0}$ is the Kronecker delta function. Note that these coefficients are constant for all initial conditions, and therefore need only be determined once. Equation (28) constitutes our final expression for the general disturbing function. In the next section we analyse the case of planets in commensurable orbits, obtain a resonant version for F_1, and discuss the averaging of the system with respect to short-period perturbations.

4 THE RESONANT HAMILTONIAN

4.1 The averaged expansion

Suppose that both planets lie in the vicinity of a generic $(p+q)/p$ mean-motion resonance, with $q \neq 0$. We define the following set of planar canonical variables

$$\begin{aligned} \lambda_1; J_1 &= L_1 + s(I_1 + I_2) \\ \lambda_2; J_2 &= L_2 - (1+s)(I_1 + I_2) \\ (1+s)\lambda_2 - s\lambda_1 - \varpi_1 = \sigma_1; I_1 &= L_1 - G_1 \\ (1+s)\lambda_2 - s\lambda_1 - \varpi_2 = \sigma_2; I_2 &= L_2 - G_2 \end{aligned} \quad (30)$$

where $s = p/q$. The last two angular variables are usually referred to as the resonant angles, and their conjugate momenta are $I_i \sim e_i^2$ (in the case of small eccentricities). Let us see how a generic periodic argument θ of F_1 appears in this new set. Introducing the passage $(M_1, M_2, \varpi_1, \varpi_2) \rightarrow (\lambda_1, \lambda_2, \sigma_1, \sigma_2)$, we obtain

$$\begin{aligned} \theta &= mM_1 - nM_2 + k\Delta\varpi \\ &= m\sigma_1 - n\sigma_2 + k(\sigma_2 - \sigma_1) + ((m(p+q) - np)Q \end{aligned} \quad (31)$$

where $qQ = \lambda_1 - \lambda_2$ is the synodic angle. Note that this implies that all periodic terms of the disturbing function are really a function of only three independent angular variables $(\sigma_1, \sigma_2, \lambda_1 - \lambda_2)$. Thus, the problem is a three-degree-of-freedom system, and the canonical moment associated to $\lambda_1 + \lambda_2$ is constant of motion. In other words

$$J_1 + J_2 = \text{const.} \quad (32)$$

We can then redefine the resonant variables (30) to include this symmetry, and express the Hamiltonian in terms of the set $(I_1, I_2, q(J_1 - J_2), \sigma_1, \sigma_2, Q)$, where $(J_1 - J_2)$ is the canonical conjugate of the synodic angle.

Our problem then has two first integrals: the Hamiltonian $F = F_0 + F_1$ and $J_{\rm tot} = J_1 + J_2$. This last function is simply the total angular momentum expressed in the new variables (see Michtchenko & Ferraz-Mello 2001). It is well known that, for all initial conditions in the vicinity of the commensurability, the frequency of Q is much higher than that of σ_i. Thus, it is common practice in these cases to average the system with respect to the synodic angle, retaining thus only those perturbations which are of long period. Introducing the notation

$$\overline{F_1} \equiv \frac{1}{2\pi} \int_0^{2\pi} F_1 \, \mathrm{d}Q \quad (33)$$

we can then average the disturbing function and thus eliminate yet another variable, reducing the system to just two degrees of freedom (I_i, σ_i). After a few algebraic manipulations, the averaged expression for the potential reads

$$\overline{F_1} = \frac{\kappa^2 m_1 m_2}{a_2} \sum_{i=0}^{3} \sum_{j=0}^{j_{\max}} \sum_{k=0}^{k_{\max}} \sum_{u=0}^{u_{\max}} \sum_{l=-l_{\max}}^{l_{\max}} \overline{R}_{i,j,k,u,l} \times (\alpha - \alpha_0)^i e_1^j e_2^k \cos(uq\sigma_1 + l(\sigma_2 - \sigma_1)) \quad (34)$$

where we have substituted the series in α by a third-order Taylor expansion around the value at exact resonance: $\alpha_0 = (1 + 1/s)^{-2/3}$. The forms of the new averaged coefficients $\overline{R}_{i,j,k,u,l}$ are easily obtained from their original definition in equation (29), substituting the resonant condition $m(p+q) - np = 0$. The upper limits of the sums, $j_{\max}, k_{\max}, u_{\max}, l_{\max}$, are user-defined and depend on the desired precision for the expansion and on the planetary eccentricities. For quasi-circular orbits, these values can be chosen as small as 2 or 4, while for highly eccentric configurations it may be necessary to adopt limits up to 15. Due to the D'Alembert properties of the disturbing function, not all the indices yield non-zero coefficients. In particular, all terms with $j < |uq - l|$ and $k < |l|$ are null, and if l is an even (odd) number, then only even (odd) values of k are relevant. The same holds for j with regards to $uq - l$.

Finally, due to the existence of the parameter $\delta > 0$, which causes our expansion to underestimate the value of the exact function near the singularities, outside the collision curve our model usually requires fewer numbers of terms (for a given precision) than the classical Laplace or Kaula expansions.

4.2 Comparisons with numerical calculations

In the following section we will apply this expansion to several resonance relations between the planets, and discuss the information the model can yield. Before this, however, it would be interesting to present a few comparisons of the final expansion (34) with numerical determination of the exact averaged disturbing function.

Typical results for the 2/1 resonance can be seen in Fig. 3 where we show the variation of $\overline{F_1}$, and its partial derivatives with respect to σ_1 and e_1, as a function of the eccentricity of the inner planet. The

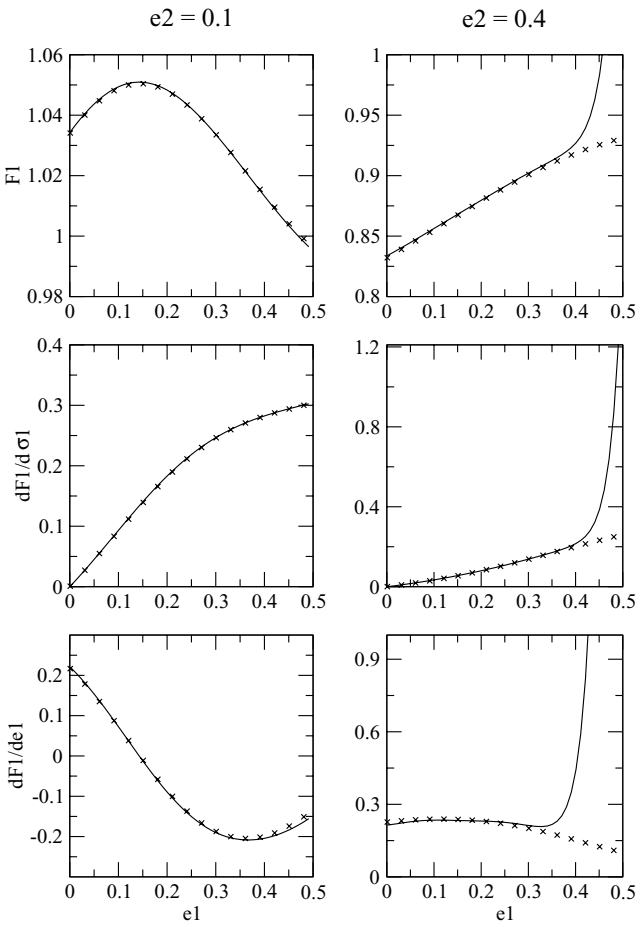

Figure 3. Variation of $|\overline{F_1}|$, and partial derivatives, as a function of e_1. Continuous lines show exact values determined numerically. Crosses indicate solutions of the model. Units are such that $\kappa = 1$.

exact function, determined numerically, is presented by the continuous lines, while the result of the expansion is shown by crosses. In all cases we have chosen $\alpha = \alpha_0$, $\sigma_1 = 90^\circ$ and $\sigma_2 = 125^\circ$. These two values for the resonant angles were chosen as a compromise between the best and worst case scenarios (i.e. farthest and closest to the collision curve). In the three plots on the left we took $e_2 = 0.1$, while the graphs on the right were obtained considering $e_2 = 0.4$.

In the first case, we can see that the agreement between both sets of data is very good, even for large values of the eccentricity of the inner planet. Both the modelled disturbing function and its derivatives reproduce the trend of the real function qualitative and quantitatively with small error. In the case of large e_2, the precision of the analytical model is still good for values of e_1 smaller than $\sim$0.3. After this, the model underestimates the magnitude of the real function. The reason for this is the existence of a singularity for $e_1 \sim 0.52$. Obviously the model cannot reproduce this behaviour, but the important characteristic is that it is still valid and yields accurate results outside the immediate vicinity of collision point.

The model can also be checked in the case of real planets in other resonant or near-resonant configurations. As an example, we present the Jupiter–Saturn system which is close to the 5:2 resonance. Although exact resonance does not exist between these planets, the mean motions of Jupiter and Saturn obey the relation $5n_{\rm Sat} - 2n_{\rm Jup} \approx 0$. Using the averaged model described in this section, we

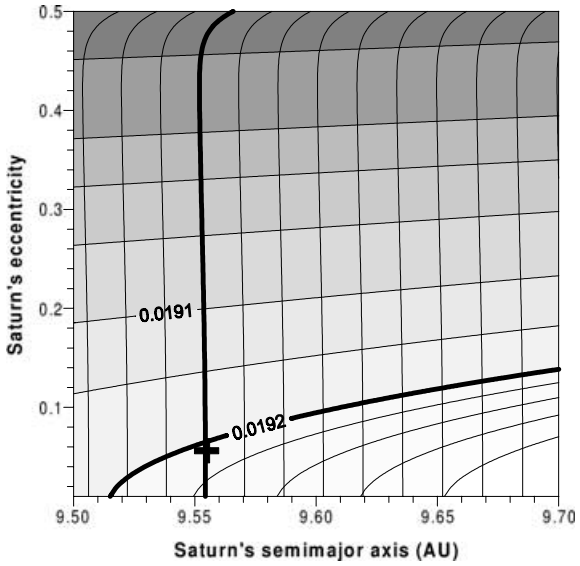

Figure 4. Energy (vertical curves) and angular momentum (horizontal curves) levels of the Jupiter–Saturn system in the (a_2, e_2) plane of the initial semimajor axis and eccentricity of Saturn. The energy and angular momentum levels shown by thick curves correspond to the actual configuration of the Jupiter–Saturn system. The location of Saturn is shown by a cross.

calculated the levels of the constant total energy and angular momentum, which are shown in Fig. 4. The energy (vertical curves) and angular momentum (inclined curves) levels are plotted in the (a_2, e_2) plane of initial semimajor axis and eccentricity of Saturn. The initial values of the semimajor axis and eccentricity of Jupiter were fixed at $a_1 = 5.2025$ au and $e_1 = 0.046$ (these values correspond to the time-averaged values of the orbital element of the Jupiter). The initial values of the critical angles were fixed at their actual values $\sigma_1 = 45.6^\circ$ and $\sigma_2 = -30.5^\circ$.

We also integrated numerically the actual Jupiter–Saturn system over 400 000 yr. The values of the total energy and angular momentum were obtained equal to $F = -0.0042143$ and $J_{\rm tot} = 0.019203$, respectively, in units of the solar mass, astronomical unit and year. The levels corresponding to these values are shown by thick curves in Fig. 4. The position of Saturn in the (a_2, e_2) plane is shown by a cross symbol. The coordinates of Saturn obtained through the numerical integration of the Jupiter–Saturn system are the time-averaged values of its orbital elements. Comparing the results of numerical and analytical modelling in Fig. 4, we note they are in very good agreement, and even far from exact resonance the model yields precise surfaces of constant energy and angular momentum.

5 APPLICATION TO THE 2/1 RESONANCE IN THE GLIESE 876 SYSTEM

In this section we apply the model to the case of the 2/1 resonance in the GJ 876 planetary system and study the main characteristics of its phase space. We begin writing the averaged resonant Hamiltonian in the form

$$F = F_0(a_1, a_2) + \overline{F}_1(a_1, a_2, e_1, e_2, \sigma_1, \sigma_2), \tag{35}$$

where the Keplerian part of the Hamiltonian, F_0, is given in equation (4) and the averaged disturbing function $\overline{F}_1$ is given in equation (34). The set of the averaged canonical variables for this resonance is given by

$$\sigma_1 = 2\lambda_2 - \lambda_1 - \varpi_1; \quad I_1 = L_1(1 - \sqrt{1 - e_1^2})$$
$$\sigma_2 = 2\lambda_2 - \lambda_1 - \varpi_2; \quad I_2 = L_2(1 - \sqrt{1 - e_2^2}) \tag{36}$$

where we recall that $L_i = m'_i\sqrt{\mu_i a_i}$ $(i = 1, 2)$, and m'_i and μ_i are the reduced planetary masses given in equation (2). The system has two integrals of motion, namely J_1 and J_2, given by

$$J_1 = L_1 + (I_1 + I_2) \quad = \text{const}$$
$$J_2 = L_2 - 2(I_1 + I_2) = \text{const}. \tag{37}$$

Note that the time variation of the planetary semimajor axes are constrained by the existence of two integrals, J_1 and J_2, and can be obtained easily through equation (37). The total angular momentum $J_{\rm tot}$ is given by a sum $J_1 + J_2$. The Hamiltonian has two degrees of freedom and the structure of its phase space can be studied through the construction of surface of section for a large set of initial conditions, such as eccentricities and critical angles.

In this section, we mainly used the Keck+Lick orbital fit of the GJ 876 system reported in Laughlin & Chambers (2001, table 3). The masses are given by $M_0 = 0.32M_{\rm Sun}$, $M_1 = 0.92M_{\rm Jup}$ and $M_2 = 3.08M_{\rm Jup}$, for the central star, inner and outer planets, respectively. The semimajor axes and eccentricities used were: $a_1 = 0.1291$ and $a_2 = 0.2067$ au; $e_1 = 0.252$ and $e_2 = 0.046$. With these numerical values we can obtain the constants of motions, $J_{\rm tot} = 0.005801$ and $J_2 = 0.004637$, in units of the solar mass, astronomical unit and year. The Hamiltonian corresponding to the current system was evaluated using equation (35) as -0.133513, which is in good agreement with the total orbital energy calculated through the direct numerical integration as -0.133552.

5.1 Energy levels in representative planes

We begin our analysis of the dynamics of the Hamiltonian system (35) by plotting, in Fig. 5, the energy level curves in the space of initial conditions. We represent the space of initial conditions in two planes. The first, shown in Fig. 5 top, corresponds to the (e_1, e_2) plane of initial eccentricities, where the initial values of the critical angles σ_1 and σ_2 are fixed at either zero or 180°. When σ_i $(i = 1, 2)$ is zero, the corresponding eccentricity e_i is denoted as positive. Conversely, e_i is written as a negative number when $\sigma_i = 180°$. The second representative plane is chosen as the (σ_1, σ_2) plane, where the planetary eccentricities are now fixed at their initial values (Fig. 5 bottom).

In the construction of the (e_1, e_2) representative plane, the choice of initial angular variables, σ_1 and σ_2, is based on previous studies of the first-order resonance (Henrard & Lemaître 1983). Indeed, outside the resonance, σ_1 and σ_2 circulate and go through either 0 or 180° for all initial conditions. Inside the 2/1 resonance, all symmetric periodic solutions of the Hamiltonian are at $\sigma_i = 0 \pmod{\pi}$ and the motion is described by oscillations about the centres located at either $\sigma_i = 0$ or $\sigma_i = 180°$ (for $i = 1, 2$). Hence, the critical angular variables can initially be fixed at 0° or 180°, without loss of generality.

The characteristic curves, along which $\dot\sigma_1 = 0$ and $\dot\sigma_2 = 0$, are shown in Fig. 5 top by large symbols. These curves can be easily obtained from conditions of periodic motion defined by

$$\frac{\partial F}{\partial I_1} = \frac{\partial F}{\partial I_2} = 0,$$

where the expression of F is given in equation (35). These curves are expected to be the seats of characteristic resonant motion (either stable or unstable librations) and their neighbourhood can be referred to as a resonance zone. For instance, the onset of zones of libration of the angles σ_i is separated from the domains of secular motion by true infinite-period separatrices.

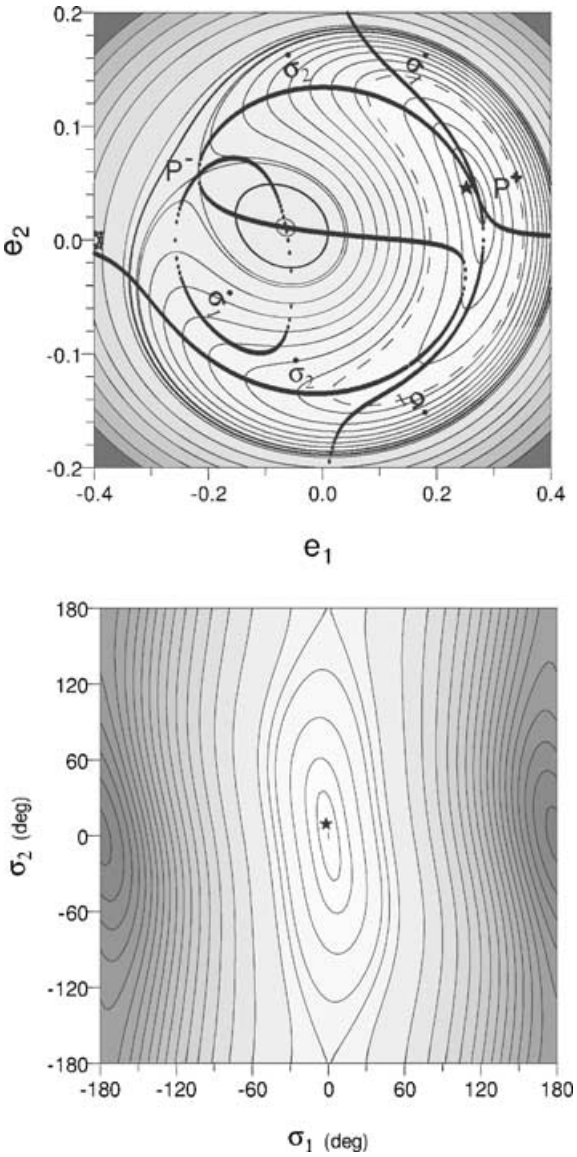

Figure 5. Top: energy level curves of the Hamiltonian given by equation (35) on the (e_1, e_2) plane of initial conditions. The signs '+' and '−' preceding the eccentricity indicate that σ_i is equal to 0 or 180°, respectively. A grey level code is used to measure energy values; the lighter regions indicate larger values of energy, whereas the darker regions indicate smaller values of energy. The equilibrium solutions of the Hamiltonian are indicated; the point P^+ is a stable equilibrium solution surrounded by a libration zone, while P^- is an unstable equilibrium solution, indicating the onset of chaos. The curves, along which $\dot\sigma_1 = 0$ and $\dot\sigma_2 = 0$, are plotted by large symbols. The current location of the GJ 876 system is shown by a star symbol. Bottom: energy levels of F on the (σ_1, σ_2) plane. The graph corresponds to planetary eccentricities equal to $e_1 = 0.252$ and $e_2 = 0.046$.

The intersections of the characteristic curves give us the location of the equilibrium solutions of the Hamiltonian on the (e_1, e_2) plane, marked by P^+ and P^- in Fig. 5 top. The nature of these solutions can be analysed on the (σ_1, σ_2) plane in Fig. 5 bottom. The angular configuration of the dynamical system characterized by maximum of energy is stable and corresponds to $\sigma_1 = 0$ and $\sigma_2 = 0$ (stable P^+-point). The opposite configuration at $\sigma_1 = \pi$ and $\sigma_2 = 0$ corresponds

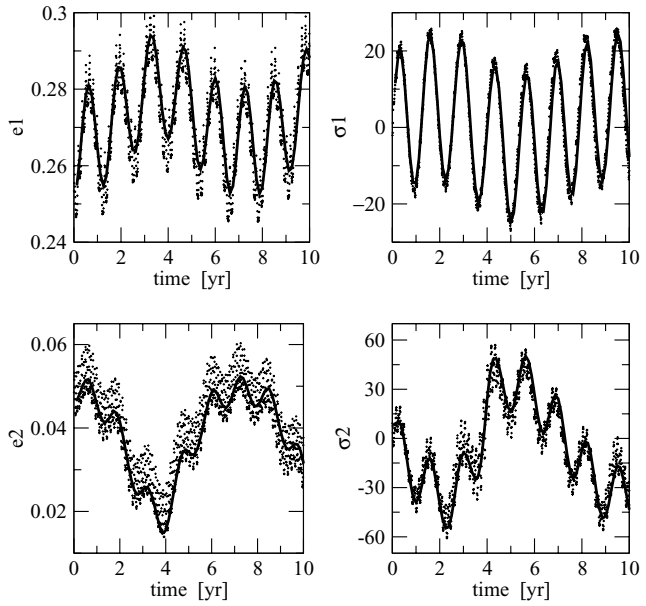

Figure 6. Temporal evolution of eccentricities and angular variables σ_1 and σ_2 for initial conditions similar to the actual GJ 876 system. Dots show the results of a numerical integration of the exact equations, while the application of the analytical model is presented by thick curves.

to minimum of energy and is unstable (unstable P^- point). The stability of the equilibrium points is defined by the behaviour of the Hessian matrix of F assessed at the point. It is worth emphasizing that, although the construction of a representative (σ_1,σ_2) plane may seem irrelevant in this case, it is important when searching for asymmetric librations (Beaugé 1994).

The current position of the GJ 876 planets in this plane is shown by a star symbol, confirming that this system is deeply inside the 2/1 mean-motion resonance, very close to a stationary solution in both resonant angles σ_1 and σ_2.

Finally, Fig. 6 shows the temporal evolution of both eccentricities and angular variables obtained with a numerical integration of the exact equations (dots). With thick curves we present the results using the model. As our Hamiltonian function has been averaged over short-period terms, the analytical data appear smoothed over all high-frequency oscillations. The overall trend, however, is practically identical in both cases.

5.2 Periodic orbits in the GJ 876 and HD 82943 systems

In Fig. 5 we have shown that it is possible to establish analytically that the GJ 876 system lies close to a stationary solution where both resonant angles librate simultaneously around zero. This configuration is sometimes called a symmetric *apsidal corotation* and, when the short-period terms are re-introduced into the Hamiltonian, they constitute stable periodic orbits.

Recently, Hadjidemetriou (2002) determined numerically the families of stable symmetric periodic orbits for both the GJ 876 and HD 82943 planetary systems, and presented his results as curves in the plane of initial eccentricities (e_1, e_2). Each point in this plane corresponds to different values of the total energy and angular momentum integrals. He noticed two different families: one occurs for $\sigma_1 = 0$ and $\sigma_2 = 180$ degrees, and the other for $\sigma_1 = 0$ and $\sigma_2 = 0$.

We can now use our model to obtain these stationary solutions and compare them to the numerical values of that paper. Results are

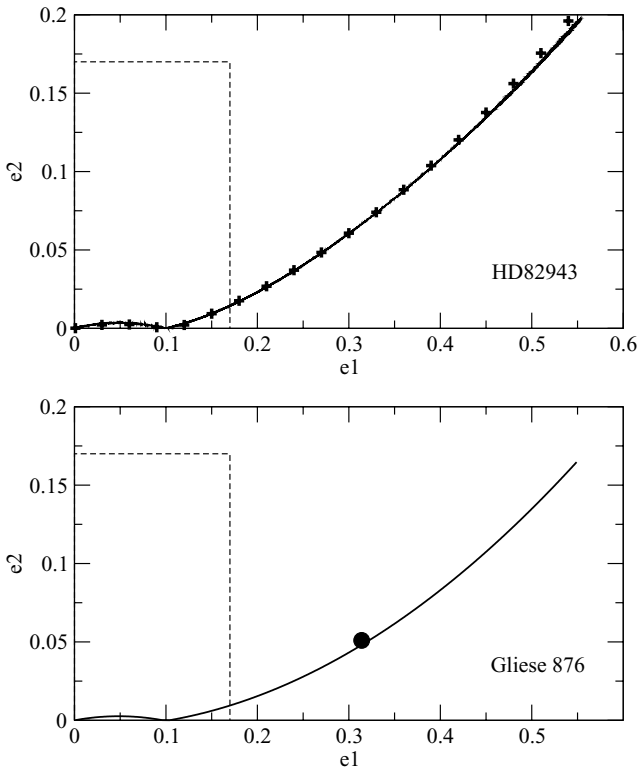

Figure 7. Families of periodic orbits for the HD 82943 and GJ 876 planetary systems. In the top graph, numerical results are shown by continuous lines, while analytical solutions are shown by crosses. In the bottom graph, the position of the GJ 876 planets is shown by a full circle. In both plots, the convergence limit of the Laplace expansion is represented by dashed lines.

presented in Fig. 7, where the top graph corresponds to the masses of the HD 82943 system, while the bottom plot shows the families of the GJ 876 planets.

In the top graph, the numerically determined periodic orbits are shown by continuous curves, while the results of our model are represented by crosses. The solutions for $\sigma_2 = 180$ are restricted in the small 'hump' seen in the region of small values of e_1, while the stationary points with $\sigma_2 = 0$ are located in the other continuous curve. With dashed lines we have drawn the convergence limit of the Laplace expansion of the disturbing function. Notice that most of the area of the plane is inaccessible to classical analytical expressions, while the model presented in this paper shows a very good agreement even for eccentricities of the order of 0.5.

In the bottom plot only the analytical results are shown (continuous lines), together with the Keck dynamical fit (Lee & Peale 2002) of the orbital elements of the GJ 876 planets (full circle). Note that the position of this system lies beyond the convergence limit of the Laplace expansion; its applicability is thus seriously compromised.

5.3 Surfaces of section

As a final example of the applications of our expansion, in this subsection we present a study of some regions of the phase space of the GJ 876 system by using the surfaces of section technique. Two sections have been chosen for the representation. The first section, corresponding to the inner planet, is a section by the plane $\sin \sigma_2 = 0$, when $\dot{\sigma}_2 < 0$, and its coordinates are $e_1 \cos \sigma_1$ versus $e_1 \sin \sigma_1$. The second section corresponds to the outer planet and is a section

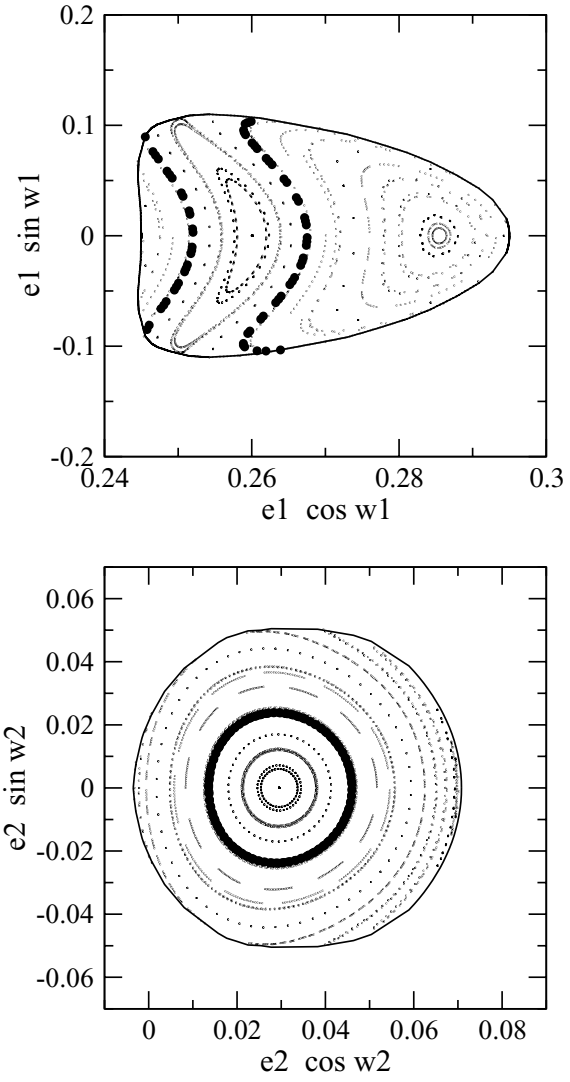

Figure 8. Top: surfaces of section of inner planet. Bottom: surfaces of section of outer plane. The sections were constructed along the energy level corresponding to the current best-fitting configuration of the GJ 876 system. The continuous curves show boundaries of the energy manifold. The sections corresponding to the actual GJ 876 system are shown by thick curves.

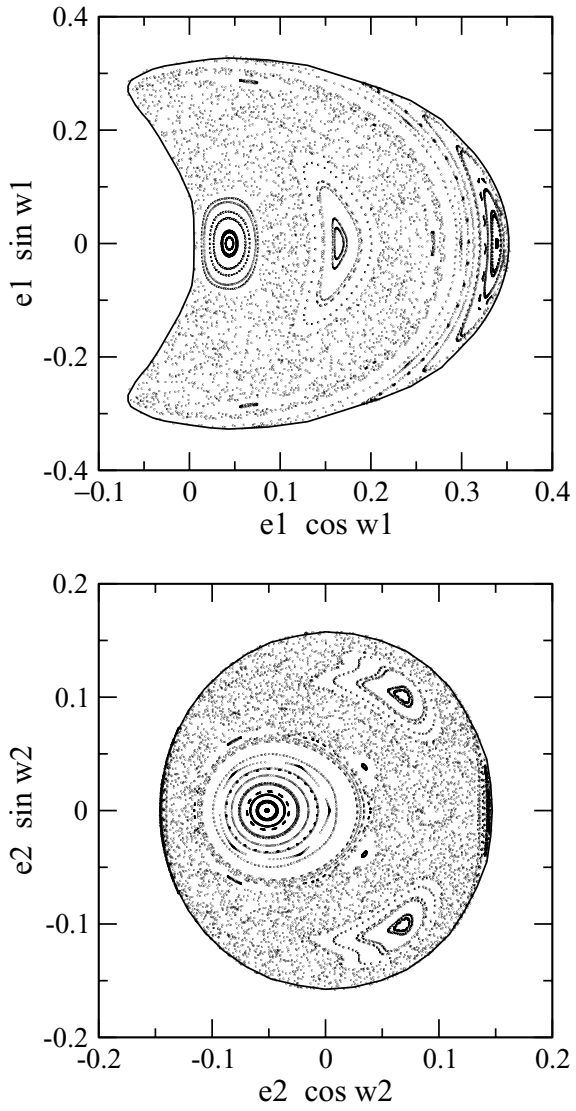

Figure 9. The same as in Fig. 8, except for the lower energy level.

by the plane $\sin \sigma_1 = 0$, when $\dot{\sigma}_1 < 0$, and its coordinates are $e_2 \cos \sigma_2$ versus $e_2 \sin \sigma_2$.

The first set of surfaces of section was calculated along the energy level $F = -0.133513$ which corresponds to the energy of the Keck+Lick dynamical fit of the planetary orbits. Fig. 8 shows the sections of the inner planet on the top panel and the sections of the outer planet on the bottom panel. The continuous curves surrounding the figure represent the boundaries of the energy manifold. We also plot by thick lines two sections on each plane which correspond to the current GJ 876 system.

For energies close to the stable equilibrium point, only the libration regime of motion is possible, and no domains of chaotic motion are seen on the sections. We can see libration islands on the inner planet section and the domain of libration of σ_2 about 0 on the outer planet section. Both critical angles are in libration about 0, although the libration trajectory of the outer planet may involve the origin on the phase space and appear kinematically as a prograde circulation. For increasing energies, the domain of the resonant regime decreases and shrinks into a stable equilibrium point at $F = -0.133508$, denoted by P^+ in Fig. 5 top.

To get an idea of the behaviour of the GJ 876 system at lower energies, we present in Fig. 9 the set of surfaces of section calculated along the energy level $F = -0.133615$ shown by the dashed curve in Fig. 5 top. In this case, the domain of the 2/1 resonance presents a complicated dynamical structure. There are three different regimes of motion and the domains of transition between them are chaotic. The main libration regime can be seen as islands of regular motion near the right-hand boundary of the energy manifold on the section of the inner planet and near the origin in the section of the outer planet. In this regime, the critical angle σ_1 remains in libration about 0, but the angle σ_2 librates now about 180°. The domains of the main libration regime are surrounded by a sea of chaotic motion. Two other regimes of motion are characterized by libration of the angle σ_1 about 0 and retrograde circulation of the angle σ_2 (and $\Delta\varpi$).

Thus, it seems that, although the present state of the planets is characterized by a very regular structure of the phase space, the same is not true for different values of the energy integral. If this system has undergone large orbital migration (which may still be in play),

then it is possible that the planets may have suffered significant chaotic evolution.

6 CONCLUSIONS

In this paper we present a new analytical expansion for the Hamiltonian of the planar planetary three-body problem, whose validity is not restricted to near-circular orbits, but is useful for very high values of the eccentricities of the massive bodies. The final expression is written as a power series of the semimajor axes and eccentricities, and cosines of the angular variables. It can be applied to any generic mean-motion commensurability between both planets or, conversely, to the non-resonant case. Through the use of modified Newcomb operators, the resulting coefficients have relatively simple recurrence relations, making their determination straightforward. In this regard, the present expansion is much more practical than that presented originally by Beaugé (1996), making it easily applicable to several physical problems in our Solar System and/or extrasolar planetary systems.

Comparisons between the model Hamiltonian and the exact (numerically averaged) function show very good precision as long as the initial conditions do not place the system in the vicinity of the collision points. Application of this expansion to the case of the 5/2 mean-motion resonance and the GJ 876 and HD 82943 extrasolar planetary systems also shows very good agreement with respect to the integrations of the exact N-body equations. Particularly, all the topological characteristics of the phase space, including equilibrium solutions, periodic orbits and temporal evolution of the orbital elements, seem to be well reproduced by our function.

It is important to recall that most extrasolar planets have orbital eccentricities above the convergence limit of the classical Laplacian disturbing function. The present expansion thus constitutes what is probably the first adequate tool with which to construct analytical models for these systems. One of its main advantages over numerical approaches is in CPU time. While the numerically determined periodic orbits shown in Fig. 7 took several hours of calculation (with a personal computer), the analytical results required only a few seconds. The construction of the surfaces of section of Figs 8 and 9 took a couple of hours with the model; a similar feat with a numerically averaged exact Hamiltonian would take several days. Of course, if only a single initial condition needs to be analysed, then a numerical integration of the exact equations is the best approach. However, extrasolar planetary orbits are many times poorly known and their masses estimated only to within a factor of $\sin I$. Thus, if a whole ensemble of initial conditions (and masses) needs to be studied, or if the aim is to identify periodic orbits of the system with many different values of energy and angular momentum, then numerical approaches tend to consume too many resources and become inviable.

Another advantage of the analytical model is that it yields results almost independent of time. For example, a numerical simulation of GJ 876 for 10 Myr yields results which are only valid for this time-span. If the integrated orbits are found to be stable, there is no guarantee that this stability will be maintained if the simulation were extended to 100 Myr, or even 20 Myr. With a Hamiltonian model on the other hand, it is possible to map the structure and topology of the phase space in the vicinity of the initial conditions, to estimate periodic orbits or regions of chaotic motion, and thus to be able to predict the dynamical behaviour of the system and stability for much longer time-scales. As the model is much faster than a simulation, it is also possible to search a large area of the phase space and map areas of orbital stability where other (undiscovered) planets may exist.

Of course, a model does not substitute an integration of the exact equations. However, it is possible to use the expansion as an exploratory tool, take advantage of its speed to find interesting and/or novel features of the system, and then confirm these results numerically.

Finally, it is important to bear in mind that the comparisons presented in this paper, with the exception of the surfaces of section, are mostly examples of previously known results. Their aim is simply to test the model and not to present novel information. Concrete applications to satellite systems and extrasolar planets exhibiting highly elliptic motions will be presented in a forthcoming paper.

The FORTRAN code developed for this model is available upon request.

ACKNOWLEDGMENTS

This work has been supported by the Brazilian National Research Council, CNPq, through the fellowships 300953/01-1 and 300946/96-1, as well as the São Paulo State Science Foundation FAPESP. The authors gratefully acknowledge the support of the Computation Centre of the University of São Paulo (LCCA-USP) for the use of their facilities.

REFERENCES

Beaugé C., 1994, Cel. Mech. Dynam. Astron., 60, 225
Beaugé C., 1996, Cel. Mech. Dynam. Astron., 64, 313
Brouwer D., Clemence G. M., 1961, Methods of Celestial Mechanics. Academic Press, New York
Butler P. et al., 2002, ApJ, 578, 565
Duriez H., 1988, A&A, 194, 309
Ellis K. M., Murray C. D., 2001, Icarus, 147, 129
Ferraz-Mello S., 1994, Cel. Mech. Dynam. Astron., 58, 37
Fischer D., Marcy G. W., Butler R. P., Laughlin G., Vogt S. S., 2002, ApJ, 564, 1028
Ford E. B., Havlikova M., Rasio F. A., 2001, Icarus, 150, 303
Hadjidemetriou J., 2002, Cel. Mech. Dynam. Astron., 83, 141
Henrard J., Lemaître A., 1983, Celest. Mech., 30, 197
Holman M. J., Murray N. W., 1996, AJ, 112, 1278
Kaula W. M., 1962, AJ, 67, 300
Laplace P. S., 1799, Mécanique Céleste (English translation by Bowditch N., 1966, Chelsea Pub. Co., New York)
Laskar J., 1991, in Roy A., ed., NATO ASI Ser. Vol. B272, Predictability, Stability and Chaos in N-Body Dynamical Systems. Plenum Press, New York, p. 93
Laskar J., Robutel P., 1995, Cel. Mech. Dynam. Astron., 62, 193
Laughlin G., Chambers J., 2001, ApJ, 551, L109
Lee M. H., Peale S. J., 2002, ApJ, 567, 596
Marcy G. W., Butler R. P., Fischer D., Vogt S. S., Lissauer J. J., Rivera E. J., 2001, ApJ, 556, 296
Michtchenko T., Ferraz-Mello S., 2001, Icarus, 149, 357
Murray N., Paskowitz M., Holman M., 2002, ApJ, 565, 608

This paper has been typeset from a TEX/LATEX file prepared by the author.